

Brain magnetic resonance image segmentation using novel improvement for expectation maximizing

Mohammad A. Balafar, PhD, MS, Abdul-Rahman Ramli, PhD, MS, Syamsiah Mashohor, PhD, MS.

ABSTRACT

الأهداف: تطوير نوعية تقسيم صور الدماغ في الرنين المغناطيسي والمتمثلة في خيار التركيب (expectation maximization)، بالإضافة إلى تقييم مدى دقة نتائج هذا التقسيم.

الطريقة: أُجريت دراسة تقسيم صور الدماغ في جامعة بوترا الماليزية، سيردونغ، ماليزيا، واستمرت خلال الفترة من فبراير إلى نوفمبر 2010م. لقد تمت دراسة الصور الحقيقية والمحاكاة للدماغ باستخدام طريقة التقسيم (EM) expectation maximization، وبعد ذلك تم عمل مقارنة بين الخوارزمية المقترحة EM1 والامتدادات المجاورة لطريقة التقسيم (FCM) (fuzzy C-mean). وطبقت الخوارزمية EM1 على 20 صورة من الصور المغناطيسية الحقيقية، وبعد ذلك تمت مقارنتها مع نتائج تقسيم صور الدماغ في الرنين المغناطيسي والتي تم تخزينها في الإنترنت.

النتائج: أشارت نتائج الدراسة إلى أن الخوارزمية EM1 قد فاقت نتائج الامتدادات المجاورة لطريقة التقسيم fuzzy C-mean وذلك في صور الدماغ المحاكاة. لقد وصل معدل قيمة مؤشر التشابه للخوارزمية المقترحة والتي جرى تطبيقها على 20 صورة حقيقية إلى 0.802، وكانت قيمة معامل جاكارد في هذه الخوارزمية أعلى من الخوارزميات الأخرى، ومقارنة لنتائج كتيب التعليمات. وقد كانت نتائج معدل قيمة جاكارد للتشابه في كافة الصور العشرين الحقيقية لكل من EM1، وامتدادات FCM: FCM ذات المعلومات الخاصة (FCM-S)، وFCM المعم السريع (FGFCM) كالتالي: EM-1=0.802, FCM-S=0.7517, enhanced FCM=0.7581, FGFCM=0.7597.

خاتمة: أظهرت النتائج مدى فعالية الخوارزمية المقترحة وتفوقها على كافة الخوارزميات الأخرى التي تمت دراستها وعلى كافة المستويات الصوتية وذلك اعتمادا على نتائج قيمة معامل جاكارد للتشابه.

Objectives: To improve the quality of expectation maximizing (EM) for brain image segmentation, and to evaluate the accuracy of segmentation results.

Methods: This brain segmentation study was conducted in Universiti Putra Malaysia in Serdong, Malaysia between February and November 2010 on simulated and real images using novel improvement for EM. The EM-1 (proposed algorithm) was compared with neighborhood based extensions for fuzzy C-mean (FCM). The EM-1 was also applied to all 20 normal real MRI volumes and compared with reported results from the Internet Brain Segmentation Repository.

Results: In simulated images, the EM-1 outperforms neighborhood based extensions for FCM. The average similarity index value of the proposed algorithm for all 20 normal images is 0.802. The EM-1 produces the average Jaccard indices ρ higher than other algorithms and near to manual results. The average similarity indices ρ for EM-1 and FCM extensions (FCM with spatial information [FCM-S], Fast Generalized FCM [FGFCM]) for all 20 normal images are: EM-1=0.802, FCM-S=0.7517, enhanced FCM=0.7581, and FGFCM=0.7597.

Conclusion: Experimental results show that the proposed algorithm performs better than other studied algorithms on various noise levels in terms of similarity index, ρ .

Neurosciences 2011; Vol. 16 (3): 242-247

From the Department of Computer & Communication Systems, Faculty of Engineering, University Putra Malaysia, Serdang, Selangor, Malaysia.

Received 25th October 2010. Accepted 13th February 2011.

Current address correspondence and reprint request to: Dr. Mohammad A. Balafar, Department of Computer Engineering, Faculty of Electrical & Computer Engineering, Tabriz University, Tabriz, Azerbaijan Shargi, Iran. Tel. +98 (411) 3848641. E-mail: balafarila@yahoo.com

The application of image processing techniques for medical imaging is rapidly increasing.¹ Most medical images are stored and represented in soft-copy.² Ultrasound, x-ray, CT, digital mammography, and MRI are the most common medical imaging types.³ An MRI can give different grey levels for different tissues and various types of neuropathology if its acquisition parameters are adjusted.⁴ Data acquisition, processing, and visualization techniques facilitate diagnosis. Medical image segmentation plays a very important role in many computer-aided diagnostic tools. These tools could save clinicians' time by simplifying complex time-consuming processes.⁵ The main part of these tools are to design an efficient segmentation algorithm. Medical images mostly contain unknown noise, in-homogeneity,⁶ and complicated structures. Therefore, segmentation of medical images is a challenging and complex task. Medical image segmentation has been an active research

area for a long time. There are many segmentation algorithms, but there is no generic algorithm for total successful segmentation of medical images.⁷ Many image techniques have been used for image segmentation, such as thresholding, region growing, statistical models, active control models, and clustering.⁷⁻¹⁰ The distribution of intensities in medical images is usually very complex, and therefore, the determination of a threshold for the images is difficult and therefore, thresholding methods have not been very successful with these images. Mostly, the thresholding method is combined with other methods. The region growing method extends thresholding by combining it with connectivity. This method requires seeds for each region, and has the same problem of thresholding for determining the suite threshold for homogeneity.⁷ Clustering methods are common for MRI brain segmentation. Expectation-maximization (EM) and fuzzy c-mean (FCM)⁸ are the most popular clustering algorithms. The Gaussian mixture model (GMM) is a popular segmentation method. The EM is used to estimate the parameters of this model. The FCM and EM only consider the intensity of images and in noisy images, intensity is not trustful. Usually, spatially adjacent pixels belong to the same cluster. Many algorithms are introduced to make FCM,^{7,9-18} and EM robust against noise, but they need to be improved. Usually, spatially adjacent pixels belong to the same cluster. Many researchers have attempted to incorporate spatial information into FCM and EM to overcome the noise problem. Zhang et al¹⁹ proposed a novel Gaussian hidden Markov Random Field (HMRF) model to integrate spatial information into the Gaussian model. They used a Markov Random Field-Maximum A Posteriori (MRF-MAP) approach to estimate the model solution. Recently, Tang et al²⁰ proposed a neighborhood-weighted GMM to overcome misclassification on the boundaries and on inhomogeneous regions of MRI brain images with noise. In this paper, a new improvement for EM is proposed, which incorporates neighborhood information into the GMM.

Standard Gaussian model. The Gaussian mixture model assumes M mixed component densities (Gaussian distribution) for each pixel (voxel) with M mixing coefficients. Each component is assigned to one target class and the goal is to obtain the class probabilities of each pixel (voxel). The probability distribution of the j th component is denoted by $p_j(x_i|\theta_j)$, where x_i is i th pixel in input image and θ_j is the parameter (mean μ_j and covariance matrix Σ_j) of component j . The probability distribution for each pixel (voxel) can be described as a mixture of probability distributions as follows:

$$p(x_i|\theta) = \sum_{j=1}^M \alpha_j p_j(x_i|\theta_j) \quad (1)$$

where α_j denotes the mixture coefficient with the constraint, $\sum_{j=1}^M \alpha_j = 1$. The probability distribution of component j is modelled by a Gaussian distribution with mean μ_j and covariance matrix Σ_j :

$$p_j(x_i|\theta_j) = p_j(x_i|\mu_j, \Sigma_j) = \frac{1}{\sqrt{\det(2\pi\Sigma_j)}} e^{-\frac{(x_i-\mu_j)^T \Sigma_j^{-1} (x_i-\mu_j)}{2}} \quad (2)$$

Usually, maximum likelihood (ML) estimation is used to find the parameters. The log-likelihood expression for the parameter θ and the image X is defined as follows:

$$\log(L(\theta|X)) = \log \prod_{i=1}^N p(x_i|\theta) = \sum_{i=1}^N \log \left(\sum_{j=1}^M \alpha_j p_j(x_i|\theta_j) \right) \quad (3)$$

Finding the ML solution from this equation is difficult. Usually, the expectation-maximization (EM) is used to obtain the parameters. The EM steps are listed in the following:

Step 1: Mean and covariance matrix are initialized using k -means and prior probability is initialized uniformly.

Step 2: Bayes' rule is used to obtain the probability of data x_i belong to class θ_j (E-step):

$$p(j|x_i, \theta^t) = \frac{\alpha_j^t p_j(x_i|\theta_j^t)}{\sum_{k=1}^M \alpha_k^t p_k(x_i|\theta_k^t)} \quad (4)$$

Step 3: Probability obtained in E-step is used to obtain the mixing coefficient, mean, and covariance matrix (M-step):

$$\alpha_j^{t+1} = \frac{1}{N} \sum_{i=1}^N p(j|x_i, \theta^t) \quad (5)$$

$$\mu_j^{t+1} = \frac{\sum_{i=1}^N x_i p(j|x_i, \theta^t)}{\sum_{i=1}^N p(j|x_i, \theta^t)} \quad (6)$$

$$\Sigma_j^{t+1} = \frac{\sum_{i=1}^N p(j|x_i, \theta^t) (x_i - \mu_j^{t+1})(x_i - \mu_j^{t+1})^T}{\sum_{i=1}^N p(j|x_i, \theta^t)} \quad (7)$$

The EM steps are repeated until convergence.

Methods. This brain segmentation study was conducted in the Universiti Putra Malaysia in Serdang, Malaysia between February and November 2010 on simulated and real images using novel improvement for EM. An improvement for the GMM is introduced by incorporating neighborhood information into

likelihood function and EM steps. In the likelihood function (equation (3)), the average of neighborhood pixels distribution is added to the distribution value of pixel x_i as neighborhood information:

$$\log(L(\theta | X)) = \log \prod_{i=1}^N p(x_i | \theta) = \sum_{i=1}^N \log \left(\sum_{j=1}^M \alpha_j^i [(1-\beta) * p_j(x_i | \theta_j^i) + \frac{\beta}{L} \sum_{r=K(i)}^{K(i+L)} p_j(x_r | \theta_j^i)] \right) \quad (8)$$

Where x_r represents a neighbor of pixel x_i and $K = 1, \dots, L$ denotes the set of neighbors, which are determined by a window centered on x_i . The L is the number of neighbors. $\frac{1}{L} \sum_{r=K(i)}^{K(i+L)} p_j(x_r | \theta_j^i)$ is the average of

distribution values for neighbor pixels. The parameter β determines the weight of neighborhood information. Incorporating neighborhood information improves the performance of clustering methods in high levels of noise, but the blurring effect degrades the performance of them in low noise levels. In order to overcome the degrading effect of algorithms in low levels of noise, the variance of noise is used to specify the weight of neighborhood information (β). The β value is set to σ , where σ is the variance of noise except for 3% noise level for which the β value is set to 0. Because in 3% noise level, the degradation effect of neighborhood incorporation is more than its improvement effect, and standard EM performs better than the improved one. An improvement for EM named EM-1 is introduced to solve likelihood function. The EM is modified as follows:

a. In equation 4, average of probability of neighborhood pixels is multiplied to the probability value of pixel x_i as neighborhood information:

$$p(j | x_i, \theta^t) = \frac{\alpha_j^i EN_{ij} p_j(x_i | \theta_j^i)}{\sum_{k=1}^M \alpha_k^i EN_{ik} p_k(x_i | \theta_k^i)} \quad (9)$$

Where EN_{ij} is the average of the probability of neighbors of x_i that belong to class θ_j :

$$EN_{ij} = \frac{1}{L} \sum_{r=K(i)}^{K(i+L)} p(j | x_r, \theta^t) \quad (10)$$

b. In equation 6, the average of neighborhood pixels values with a weight is added to each pixel as neighborhood information:

$$\mu_j^{t+1} = \frac{\sum_{i=1}^N ((1-\beta) * x_i + \frac{\beta}{L} \sum_{r=K(i)}^{K(i+L)} x_r) p(j | x_i, \theta^t)}{\sum_{i=1}^N p(j | x_i, \theta^t)} \quad (11)$$

c. In equation 7, the average of distance of neighbor pixel from component center is added to the distance of pixel from component center as neighborhood information:

$$\Sigma_j^{t+1} = \frac{\sum_{i=1}^N p(j | x_i, \theta^t) ((x_i - \mu_j^{t+1})(x_i - \mu_j^{t+1})^T + \frac{\beta}{L} \sum_{r=K(i)}^{K(i+L)} (x_r - \mu_j^{t+1})(x_r - \mu_j^{t+1})^T)}{\sum_{i=1}^N p(j | x_i, \theta^t)} \quad (12)$$

In an MRI image, noise behaves in a Rician distribution.²¹ Noise distribution approaches Gaussian with increasing Signal to Noise Ratio (SNR) and approaches Rayleigh with decreasing SNR. The Rician distribution in the background is Rayleigh distributed, because the signal is usually considered as zero and the probability distribution function (PDF) becomes as follows:

$$p(O_i) = \frac{O_i}{\sigma^2} e^{-O_i^2/(2\sigma^2)} \quad (13)$$

Where $O = 1, \dots, n$ is the set of observations in the background. The variance of noise can be estimated by equation 14:²¹

$$\sigma_{Noise}^2 = \frac{1}{2n} \sum_{i=1}^n O_i^2 \quad (14)$$

Sometimes in real images, the background has no noise. In this case, the parameter β is considered 3 because the real images usually contain the noise.

Results. The proposed extension of EM (EM-1) is simulated and applied on the simulated images from BrainWeb,²² and real images from the Internet Brain Segmentation Repository (IBSR).²³ The results of the proposed algorithm are compared with results for the existing extensions of EM²⁴ (DPM, rjMCMC, KVL, MPM-MAP), the existing neighborhood based extension of FCM (FCM_S,²⁵ FGFCM²⁵) and reported results in IBSR. The results of algorithms are compared quantitatively to analyze their performance. The neighborhood size, N for the proposed algorithm is set to 3×3 . The similarity index²⁴ is used to evaluate the algorithms quantitatively. The similarity index ρ is the degree of a class of pixels matching between ground truth and segmentation result. It is defined as:

$$\rho = \frac{2 |X_i + Y_i|}{|X_i| + |Y_i|} \quad (15)$$

where X_i represents class i in ground truth and Y_i represents the same class in the segmentation result.

Simulated images. The simulated MRI images are obtained from BrainWeb. A simulated data volume with T1-weighted sequence, slice thickness of 1 mm, and a volume size of $217 \times 181 \times 181$ is used. Non-

brain tissues are removed prior to segmentation. The number of tissue classes in the segmentation is set to 3: grey matter (GM), white matter (WM), and CSF. It should be noted that background pixels are ignored in this experiment. In order to compare different clustering algorithms, they are applied on whole volume at different noise levels, and average similarity is used to compare them. The average similarity indices ρ for clustering algorithms are shown in Figure 1. The EM-1 has similarity indices higher than other algorithms. The EM-1 (proposed algorithm) is compared with neighborhood based extensions for FCM. Figure 2 shows the average similarity indices ρ for EM1 and FCM extensions (FCM_S and FGFCM) when they are applied on 3D volume at different noise levels. Figure 2 shows that EM-1 has the highest similarity indices. Afterwards, the effect of different neighborhood sizes on the performance of proposed algorithms is analyzed. The proposed algorithm with different neighborhood sizes is applied on 3D volume, and again the average similarity is used to analyze the effect of different neighborhood sizes on the proposed algorithm. The average similarity index ρ of the proposed algorithm

when different neighborhood sizes (3, 5, and 7) are applied on the simulated image with 9% noise are: 0.9085, 0.904, and 0.894.

Real images. The proposed algorithm is also applied on real MRI images. The real MRI images are obtained from the IBSR by the Centre for Morphometric Analysis, Massachusetts General Hospital. Twenty normal data volume with T1-weighted sequence were used.

In the IBSR, manual segmentation results are provided along with brain MRI data to encourage introducing new segmentation algorithms and evaluate their performance. Trained investigators used semi-automated histograms on the spatially normalized images to obtain manual segmentation. Prior to clustering, inhomogeneity correction along with intensity adjusting is applied to real image volumes. First, the EM-1 (proposed algorithm) is applied to slices of a real MRI volume with size 256x256x65 and the similarity index ρ for each slice is presented. Figure 3 shows the similarity indices of the proposed algorithm for every slice of the MRI volume. The EM-1 (proposed algorithm) is also applied to all 20 normal real MRI volumes and compared with reported results from the IBSR. Figure 4 shows the similarity index of the

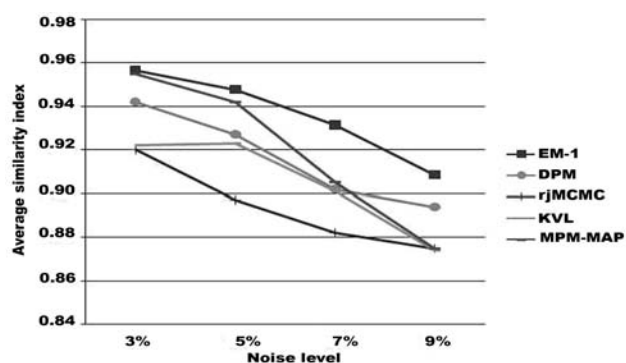


Figure 1 - The average similarity indices for proposed algorithm (EM-1) and several EM based methods (EM, DPM, rjMCMC, KVL, and MPM-MAP) on different noise levels.

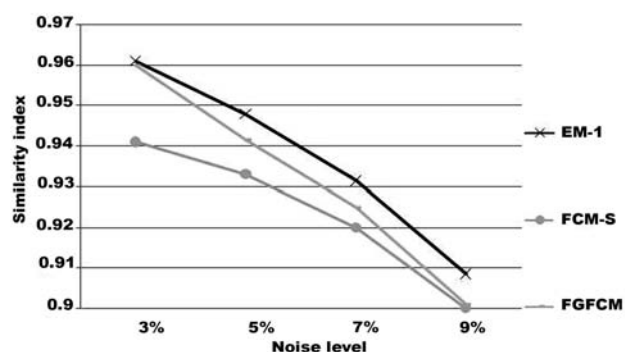


Figure 2 - The average similarity indices for the proposed algorithm (EM-1) and several FCM extensions (FCM-S and FGFCM) on different noise levels.

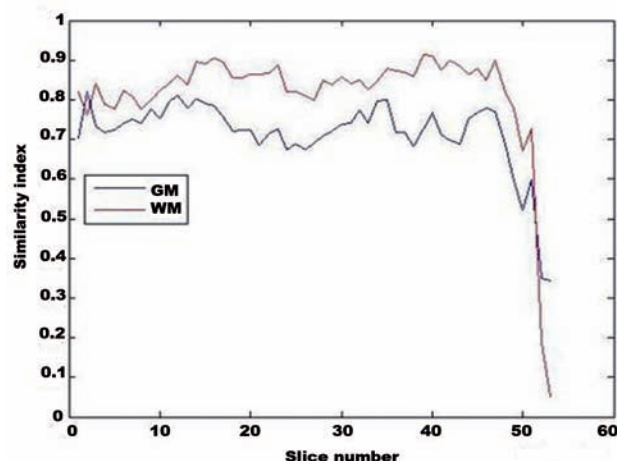


Figure 3 - The similarity index of the proposed algorithm when applied to real images. GM - grey matter, WM - white matter

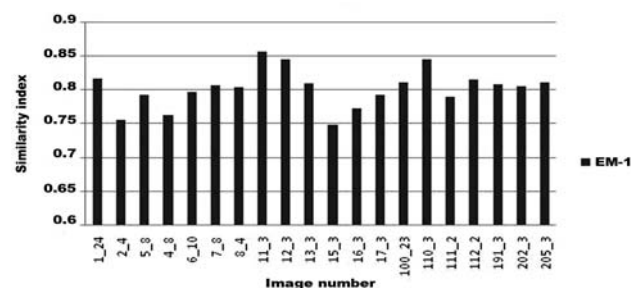


Figure 4 - The similarity index of the proposed algorithm (EM-1) when applied on 20 real images.

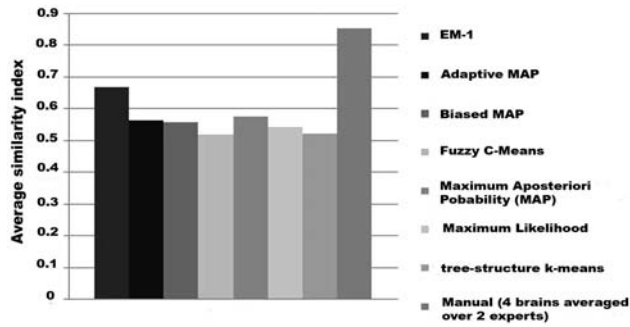


Figure 5 - The average Jaccard index of the proposed algorithm (EM-1) and reported results for several methods from the Internet Brain Segmentation Repository when applied on 20 real images.

proposed algorithm (EM-1) when it is applied on each of 20 normal image volumes. The average similarity index value of the proposed algorithm for all 20 normal images is 0.802. The reported results are based on the Jaccard index.²⁶ Therefore, the average Jaccard index values of algorithms for 20 normal real MRI volumes are used to evaluate them. Figure 5 shows the average Jaccard index values of different algorithms for all 20 normal images.

Discussion. To evaluate EM-1, the method is compared with existing neighborhood based extensions for EM on the whole volume of simulated images at different noise levels. The EM-1 has similarity indices higher than other algorithms, and when the noise level is increased, its similarity indices decrease more slowly than others. The EM-1 (proposed algorithm) is also compared with neighborhood-based extensions for FCM (FCM_S and FGFCM) when they are applied on 3D simulated volume at different noise levels. The EM-1 has the highest similarity indices. Following this, the effect of different neighborhood sizes on the performance of proposed algorithms was analyzed. When the neighborhood size is increased, the similarity indexes of the proposed algorithm decreases. The proposed algorithm was also applied to real MRI images obtained from the IBSR. The EM-1 (proposed algorithm) is applied to all 20, 3D normal real MRI volumes and compared with reported results from IBSR. The average similarity index value of the proposed algorithm (EM-1) for all 20 normal images is 0.802. The EM-1 produces the average Jaccard indices ρ higher than other algorithms. The EM-1 is also compared with neighborhood based extensions for FCM. The average similarity indices ρ for EM-1 and FCM extensions (FCM_S, FCM-EN, FGFCM) for all 20 normal images are: EM-1=0.802, FCM-S=0.7517, FCM-EN=0.7581, FGFCM=0.7597. The EM-1 produced the highest similarity indices.

In conclusion, an improvement for EM has been introduced. In order to overcome the problem of standard EM in the presence of noise, the introduced algorithms are formulated by modifying the equations of the standard EM algorithm, which allow the neighborhood pixels to be incorporated in the labeling of a pixel. The introduced algorithm is tested on simulated MRI images, with different noise levels, and real images. The performance of the existing neighborhood based EM, and FCM algorithms and the proposed algorithm are compared qualitatively. The similarity index, ρ of the segmentation results is used to evaluate different algorithms. Experimental results show that the proposed algorithm performs better than other studied algorithms on various noise levels in terms of the similarity index, ρ .

In the future, we will consider undertaking research on other kinds of clustering methods to improve their functionality. Also, we will analyze the effects of different clustering methods in segmentation of medical images for the diagnosis of abnormal or various important matters in medical images.

References

- Balafar MA, Ramli AR, Mashohor S. Edge-preserving Clustering Algorithms and Their Application for MRI Image Segmentation. In: Ao SI, Castillo O, Douglas C, Feng DD, Lee JA, editors. Proceedings of the International MultiConference of Engineers and Computer Scientists IMECS 2010; 2010 March 17-19; Hong Kong. Hong Kong: IAENG; 2010. p. 17-19.
- Chang PL, Teng WG. Exploiting the self-organizing map for medical image segmentation. Proceedings of the Twentieth IEEE International Symposium on Computer-Based Medical Systems; 2007 Jun 20-22; Slovenia. Slovenia: IEEE; 2007. p. 281-288.
- Jan J. Medical image processing, reconstruction, and restoration: concepts and methods. 1st ed. Brno (Czech): Taylor & Francis, CRC; 2006. p. 760.
- Tian D, Fan L. A Brain MR Images Segmentation Method Based on SOM Neural Network. Proceedings of the 1st International Conference on Bioinformatics and Biomedical Engineering; 2007 July 6-8; Wuhan. Wuhan (China): IEEE; 2007. p. 686-689.
- Jiang Y, Meng J, Babyn P. X-ray image segmentation using active contour model with global constraints. Proceedings of CIISP 2007; 2007 June 4; Honolulu. Honolulu (HI): IEEE; 2007. p. 240-45.
- Balafar MA, Ramli AR, Mashohor S. A new method for MR grayscale inhomogeneity correction. *Artificial Intelligence Review* 2010; 34: 195-204.
- Balafar MA, Ramli AR, Saripan MI, Mashohor S. Review of brain MRI image segmentation methods. *Artificial Intelligence Review* 2010; 33: 261-274.
- Balafar MA, Ramli AR, Mashohor S. Compare different spatial based Fuzzy C-Mean (FCM) extensions for MRI Image Segmentation. Proceedings of the ICCAE 2010; 2010 April 19. Singapore. Singapore: IEEE; 2010. p. 609-611.

9. Balafar MA, Ramli AR, Saripan MI, Mahmud R, Mashohor S. Medical image segmentation using fuzzy C-Mean (FCM), learning vector quantization (LVQ) and user interaction. *Communications in Computer and Information Science* 2008; 15: 177-184.
10. Balafar MA, Ramli AR, Saripan MI, Mashohor S, Mahmud R. Improved Fast Fuzzy C-Mean and its Application in Medical Image Segmentation. *Journal of Circuits, Systems, and Computers* 2010; 19: 203-214.
11. Zou K, Wang Z, Hu M. An new initialization method for fuzzy c-means algorithm. *Fuzzy Optimization and Decision Making* 2008; 7: 409-416.
12. Su HR, Liou M, Cheng PE, Aston JAD, Chuang CH. MR image segmentation using wavelet analysis techniques [CD-ROM]. *Neuroimage* 2005; 26 (Suppl 1).
13. He R, Datta S, Sajja BR, Narayana PA. Generalized fuzzy clustering for segmentation of multi-spectral magnetic resonance images. *Comput Med Imaging Graph* 2008; 32: 353-366.
14. Balafar MA, Ramli AR, Saripan MI, Mashohor S, Mahmud R. Medical Image Segmentation Using Fuzzy C-Mean (FCM) and User Specified Data. *Journal of Circuits, Systems, and Computers* 2010; 19: 1-14.
15. Balafar MA, Ramli AR, Saripan MI, Mahmud R, Mashohor S. Medical image segmentation using anisotropic filter, user interaction and fuzzy C-Mean (FCM). *Communications in Computer and Information Science* 2008. 15: 169-176.
16. Balafar MA, Ramli AR, Saripan MI, Mahmud R, Mashohor S. Medical image segmentation using fuzzy C-mean (FCM) and dominant grey levels of image. Proceedings of the Visual Information Engineering Conference; 2008 July 29; Xian, China: IET; 2008. p. 314-317.
17. Balafar MA, Ramli AR, Saripan MI, Mahmud R, Mashohor S. Medical image segmentation using fuzzy C-mean (FCM), Bayesian method and user interaction. Proceedings of the International Conference on Wavelet Analysis and Pattern Recognition; 2008 Aug 30; Hong Kong, China: IEE; 2008. p. 68-73.
18. Balafar MA, Ramli AR, Saripan MI, Mahmud R, Mashohor S. New multi-scale medical image segmentation based on fuzzy c-mean (FCM). Proceedings of the IEEE conference on innovative technologies in intelligent systems and industrial applications; 2008 July 12; Cyberjaya, Malaysia: IEEE; 2008. p. 66-70.
19. Zhang Y, Brady M, Smith S. Segmentation of brain MR images through a hidden Markov random field model and the expectation-maximization algorithm. *IEEE Trans Med Imaging* 2001; 20: 45-57.
20. Tanga H, Dillensegerb JL, Baoa XD, Luo LM. A vectorial image soft segmentation method based on neighborhood weighted Gaussian mixture model. *Comput Med Imaging Graph* 2009; 33: 644-650.
21. He L, Greenshields IR. A nonlocal maximum likelihood estimation method for Rician noise reduction in MR images. *IEEE Trans Med Imaging* 2009; 28: 165-172.
22. Cocosco CA, KollokianV, Kwan RKS, Evans AC. BrainWeb: Online Interface to a 3D MRI Simulated Brain Database [Internet]. The Montreal Neurological Institute: McGill University; 1997 May 1 [updated 2006 Jun 12; Cited 2010 October 1]. Available from URL: www.bic.mni.mcgill.ca/brainweb/.
23. MGH CMA. IBSR: The Internet Brain Segmentation Repository [Internet]. National Institute of Science: Harvard Medical School; 1997 [updated 2009 January 15; Cited 2010 October 1]: Available from URL: <http://www.cma.mgh.harvard.edu/ibsr/>.
24. Ferreira da Silva AR. Bayesian mixture models of variable dimension for image segmentation. *Computer Methods Programs Biomed* 2009; 94: 1-14.
25. Cai W, Chen S, Zhang D. Fast and robust fuzzy c-means clustering algorithms incorporating local information for image segmentation. *Pattern Recognition* 2007; 40: 825-838.
26. Vovk U, Pernus F, Likar B. A review of methods for correction of intensity inhomogeneity in MRI. *IEEE Tran Med Imaging* 2007; 26: 405-421.

ETHICAL CONSENT

All manuscripts reporting the results of experimental investigations involving human subjects should include a statement confirming that informed consent was obtained from each subject or subject's guardian, after receiving approval of the experimental protocol by a local human ethics committee, or institutional review board. When reporting experiments on animals, authors should indicate whether the institutional and national guide for the care and use of laboratory animals was followed. Research papers not involving human or animal studies should also include a statement that approval/no objection for the study protocol was obtained from the institutional review board, or research ethics committee.